

## 3D UNSTEADY TURBULENT FLOW ANALYSIS IN A FRANCIS TURBINE RUNNER AT NOMINAL AND OFF-DESIGN OPERATING CONDITIONS

PHAM THI KIM LOAN, BUI VAN GA  
*University of Danang*

**ABSTRACT.** This paper presents the use of a commercial Navier-Stokes turbulent flow code (FLUENT) as a mean to evaluate the behavior of a Francis turbine runner for the design and off-design conditions. The flow in the runner is analyzed numerically at different operating points. The numerical results permit to observe physical phenomena in the runner that are important in the process of hydraulic turbo machinery design. Values of different velocity components in the flow, blade pressure distribution... given by the model are compared with experimental data at nominal and off-design flow conditions. Computer resource involves in the flow analysis should be compatible with the need of design process of a runner. Therefore 12 hours of CPU time can be considered as acceptable for calculating at each operating point on a computer workstation of medium size power.

### 1 Introduction

Numerical flow simulations in a runner of hydraulic turbines now are very frequent. This paper presents the capacity of the FLUENT software for modelisation of flow in a runner at nominal and different off-design operating conditions.

In this study, the FLUENT software using a  $k$ - standard turbulent model, is used to analyze the behavior of the runner designed by Neyrpic. It is also used for experimental research work in the laboratory LEGI, INPG (Institut National Polytechnique Grenoble). To enhance the accuracy of the prediction, it is necessary to calculate the 3D flow at both steady and unsteady states. However the transient calculations in a complete turbine runner with a large number of nodes requires too much computational effort to be practicable. Therefore this method consists in modeling and computing the 3D flow for different operating points in a single channel of the 13-blade runner with periodicity assumed between the channels of the turbine.

After control of numerical convergence, comparison between experimental data and numerical results of the specific energy and momentum is proposed. The physical coherence is shown with many operating points. The unsteady calculation gives the results more accurate than those of the steady simulation, however it requires more CPU time for the numerical convergence.

## 2 Tools and geometry

### 2.1 Turbulent models and boundary conditions

For all the calculations, the Navier-Stokes turbulent viscous flow code (the commercial code FLUENT) is used. It is a finite volume code with a lot of available turbulent models. The equation for conservation of mass can be written as:

$$\frac{\partial \rho}{\partial t} + \frac{\partial}{\partial x_i} (\rho u_i) = 0, \quad (2.1)$$

where  $\rho, u$ : the density (net mass) and the velocity;  $i(x, y, z)$ : the coordinate system's directions.

Conservation of momentum in the  $i$ -th direction in an inertial (non accelerating) reference frame is described by the equation:

$$\frac{\partial (\rho u_i)}{\partial t} + \frac{\partial}{\partial x_j} (\rho u_i u_j) = -\frac{\partial p}{\partial x_i} + \frac{\partial \tau_{ij}}{\partial x_j} + \rho g_i + F_i, \quad (2.2)$$

where  $p$  is the static pressure,  $\tau_{ij}$  is the stress tensor,  $\rho g_i$  and  $F_i$  are the gravitational body force and external body force in the  $i$ -th direction respectively. The stress tensor is given by the following formula:

$$\tau_{ij} = \mu \left( \frac{\partial u_i}{\partial x_j} + \frac{\partial u_j}{\partial x_i} \right) - \frac{2}{3} \mu \frac{\partial u_l}{\partial x_l} \delta_{ij}, \quad (2.3)$$

where  $\mu$  is the molecular viscosity and the second term on the right side is the effect of volume dilation.

Substituting Reynolds decomposition  $u_i = \bar{u}_i + u'_i$  into the Navier-Stokes equation, we have the same general form with the velocities and other solution variables now presenting averaged values. The additional terms that present the effects of turbulence  $-\rho \overline{u'_i u'_j}$  appear in the averaged momentum equation. These Reynolds stresses must be modeled in order to close the average equations:

$$\begin{aligned} \frac{\partial \rho}{\partial t} + \frac{\partial}{\partial x_i} (\rho \bar{u}_i) &= 0, \\ \rho \frac{\partial \bar{u}_i}{\partial t} &= -\frac{\partial \bar{p}}{\partial x_i} + \frac{\partial}{\partial x_j} \left[ \mu \left( \frac{\partial \bar{u}_i}{\partial x_j} + \frac{\partial \bar{u}_j}{\partial x_i} - \frac{2}{3} \delta_{ij} \frac{\partial \bar{u}_l}{\partial x_l} \right) \right] + \\ &+ \frac{\partial}{\partial x_j} \left( -\rho \overline{u'_i u'_j} \right) + \rho g_i + F_i. \end{aligned} \quad (2.4)$$

A common method employs the Boussinesq hypothesis (used in the Spalart-Allmaras model and the  $k - \varepsilon$  model) to relate the Reynolds stresses to the mean velocity gradients:

$$-\rho \overline{u'_i u'_j} = \mu_t \left( \frac{\partial \bar{u}_i}{\partial x_j} + \frac{\partial \bar{u}_j}{\partial x_i} \right) - \frac{2}{3} \left( \rho k + \mu_t \frac{\partial \bar{u}_l}{\partial x_l} \right) \delta_{ij}, \quad (2.5)$$

where  $\mu_t$  is the turbulent viscosity. According to JONES and LAUNDER [3]:

$$\mu_t = \rho C_\mu \frac{k^2}{\varepsilon} \quad \text{where} \quad k = \frac{1}{2} \sum_{i=1}^3 \overline{u_i'^2}; \quad \varepsilon = \nu \overline{\frac{\partial u_i'}{\partial x_j} \frac{\partial u_i'}{\partial x_j}}. \quad (2.6)$$

The turbulent kinetic energy  $k$ , and the turbulence dissipation rate  $\varepsilon$  are described by the equations:

$$\begin{aligned} \rho \left\{ \frac{\partial k}{\partial t} + \overline{u_j} \frac{\partial k}{\partial x_j} \right\} &= \frac{\partial}{\partial x_j} \left( \left( \mu + \frac{\mu_t}{\sigma_k} \right) \frac{\partial k}{\partial x_j} \right) + P - \rho \varepsilon, \\ \rho \left\{ \frac{\partial \varepsilon}{\partial t} + \overline{u_j} \frac{\partial \varepsilon}{\partial x_j} \right\} &= \frac{\partial}{\partial x_j} \left( \left( \mu + \frac{\mu_t}{\sigma_\varepsilon} \right) \frac{\partial \varepsilon}{\partial x_j} \right) + C_{\varepsilon 1} \frac{\varepsilon}{k} P - \rho C_{\varepsilon 2} \frac{\varepsilon^2}{k}, \end{aligned} \quad (2.7)$$

where

$$P = \mu_t \left( \frac{\partial \overline{u_i}}{\partial x_j} + \frac{\partial \overline{u_j}}{\partial x_i} \right) \frac{\partial \overline{u_i}}{\partial x_j},$$

$$C_\mu = 0,09 ; \sigma_k = 1,00 ; \sigma_\varepsilon = 1,30 ; C_{\varepsilon 1} = 1,44 ; C_{\varepsilon 2} = 1,92 .$$

Two additional transport equations (2.7) for the turbulent kinetic energy  $k$ , and the turbulence dissipation rate  $\varepsilon$  are solved and  $\mu_t$  is computed as a function of  $k$  and  $\varepsilon$ . The standard  $k - \varepsilon$  model is well valid only for the fully turbulent flows. Therefore in this study the turbulent model used is the standard  $k - \varepsilon$  with logarithmic wall laws.

FLUENT provides the ability to calculate streamwise-periodic fluid flow. This flow is encountered in a variety of applications, including flows across turbo machinery. In such flow configurations, the geometry varies in a repeating manner along the direction of the flow leading to a periodic fully-developed flow regime in which the flow pattern repeats in successive cycles.

In this work, the flow in a channel of the 13-blade turbine runner is calculated by FLUENT. The channel grid (Fig.1) of this simulation contains 75113 elements including 71900 tetrahedrons, 2856 hexahedrons and 357 prisms. This method permits to use the boundary conditions as outlet with radial equilibrium pressure distribution; lateral faces with periodic conditions in order to reduce calculation domain; shroud, hub and the blade with wall condition and inlet with the boundary condition extrapolated from the results of the calculation for the runner guide vane interaction [1], [5].

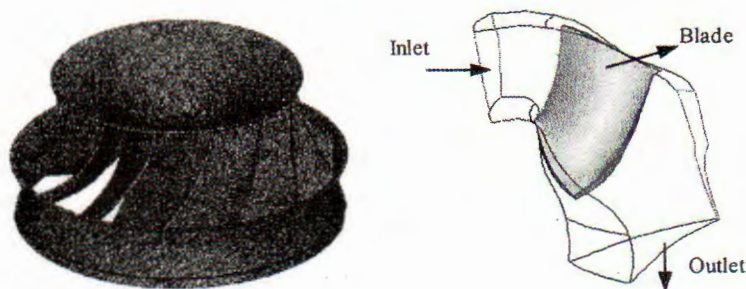


Fig. 1. The turbine runner and the single channel



Many important engineering flows involve swirl or rotation and FLUENT is well-equipped to model such flows. Rotating flows are encountered in turbo machinery. The flow involves a rotating boundary which moves through the fluid (for example an impeller blade) so we need to use a rotating reference frame to model the problem.

Because the rotation defined by the boundary conditions can lead to a large complex forces in the flow, the FLUENT calculations will be less stable as the speed of rotation increases. Hence, one of the most effective control is to solve the rotating flow problem starting with a low rotational speed and then slowly increase it up to the desired level.

## 2.2 Numerical scheme

FLUENT allows us to choose either of two numerical methods: coupled solver and segregated solver. The last one is used in our calculations. Using the segregated solver, the governing equations are solved sequentially (segregated from one another). In both the segregated and coupled solution methods, the non-linear governing equations are linearized to produce a system of aligns for the dependent variables in every computational cell. The resultant linear system is solved to yield an updated flow-field solution. The manner in which the governing equations are linearized may take an implicit or explicit form with respect to the set of dependent variables. In the segregated solution method each discrete governing equations is linearized implicitly. In summary, the segregated approach solves for a single variable field by considering all cells simultaneously. It then solves for the next variable field by again considering all cells at the same time, and so on.

## 2.3 Discretisation

FLUENT uses a control-volume-based technique to convert the governing equations to the algebraic equations that can be solved numerically. FLUENT stores discrete values of the scalar  $\phi$  at the cell center. However, values of  $\phi$  converted through the faces are required for the convection terms in the discrete aligns and must be interpolated from the cell center values. This is accomplished using an upwind scheme. FLUENT allows us to choose from several schemes: first-order upwind, second-order upwind, power law and QUICK. In this work, the second-order upwind is selected.

## 3 Calculation process and time

Eight calculations for different operation points are needed for one aperture angle of the runner guide vane and the calculations are performed with both the steady and unsteady solutions. These eight operating points of the turbine correspond to the experimental conditions including 1 nominal and 7 off-design points (3 overfull load points, 3 partial load points and the runaway point that is the extremely dangerous operating condition with minimal measured efficiency value and torque null). The parameters of these points such as the fluid head, the flow, the rotational speed, the moment are obtained by experiment. The values of the flow and the rotational speed are using for the boundary conditions and the moment as a creteria for the calculation evaluation. These parameters are shown in Table 1.

Table 1

	Off-design-Overfull load			Nominal	Off-design-Partial load		
$\varphi$	0.51	0.47	0.42	0.38	0.32	0.28	0.21 (runaway)
$\omega$ (rad/s)	51.49	56.38	62.32	69.94	82.77	96.53	123.11
$\Psi$	2.22	1.85	1.52	1.2	0.86	0.63	0.39

In Table 1, each operating point is characterized by two non-dimensional parameters defined as:  $\varphi = \frac{Q}{\pi \cdot \omega \cdot R_{2e}^3}$ : Coefficient of flow rate and  $\psi = \frac{2gH}{\omega^2 \cdot R_{2e}^2}$ : Coefficient of specific energy. where  $Q, H, \omega, R_{2e}$  are respectively related to the flow rate, the fluid head ( $H=3\text{m}$  for this simulation), the rotational speed and the specific radius of the runner ( $R_{2e}=100\text{ mm}$ ).

Simulations were made on the Silicon Graphics Type 02 work station with 256 MB of memory. The calculation time for an unsteady solution varied from 12 hours for the nominal point to 120 hours for the runaway.

Since the FLUENT formulation is fully implicit, there is no stability criterion that needs to be met in determining the time step. However, to model transient phenomena properly, it is necessary to set  $\Delta t$  at least one order of magnitude smaller than the time constant in the system being modeled. Therefore the time step chosen in this simulation corresponds to the rotation of the runner for 1 degree (0,00025s at nominal).

The last flow solution calculated for one calculation is always used as initial approximation for the next one. Calculation times then reduce with the number of iterations because the global flow solution approaches convergence. At the end of each solver iteration, the residual sum for each of the variables is computed and stored.

#### 4 Results and discussion

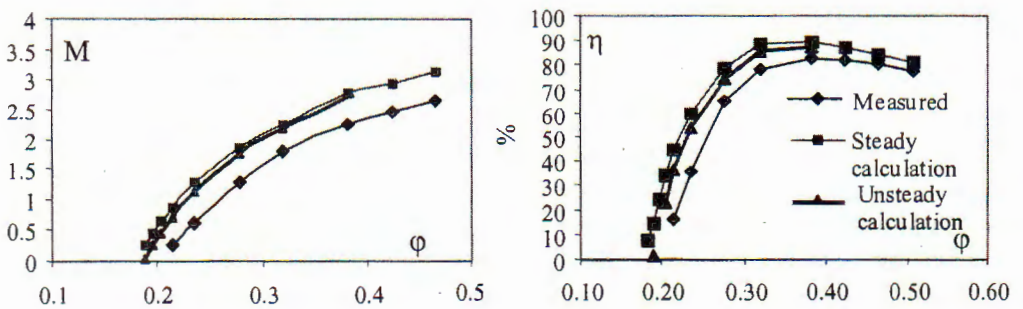


Fig. 2. Evolution of Moment and Efficiency



After control of numerical convergence of the flow rate, the components of velocity, the turbulent kinetic energy  $k$  and the turbulence dissipation rate  $\epsilon$ , comparison between experimental data and numerical results obtained with FLUENT are proposed. The physical coherence is shown with the moment criteria. Other comparisons are made on the experimental values of the velocity components at the outlet section. The analysis of the numerical results is in agreement with the experimental ones. The blade loading (moment) is well calculated in which the results of the unsteady formulations are more accurate (Fig. 2).

The calculation gives correct results [1], [7]. In particular the moment is well predicted as nearly null torque at runaway (Fig. 2). We can clearly see the capability of the code in simulation of the flow in a Francis turbine at nominal and off-design operating conditions. The error becomes higher at the overfull load points, i. e. from the nominal point. For the value of moment, the calculation error (14,77% maximal) caused by the hydraulic and mechanical losses in the volute, the distributor and the diffuser since these parts are not including in the calculation domain. The pressure distribution on both sides of the blade is illustrated in the Figs.3 and 4. At nominal the pressure distribution on both faces of blade is regular (Fig.3a, 4a) while at runaway, an inversion of the blade charging is observed on the leading edge (Fig.4b) and nearby the shroud zone (Fig.3b). The stress state of the runner is particularly important at runaway point.

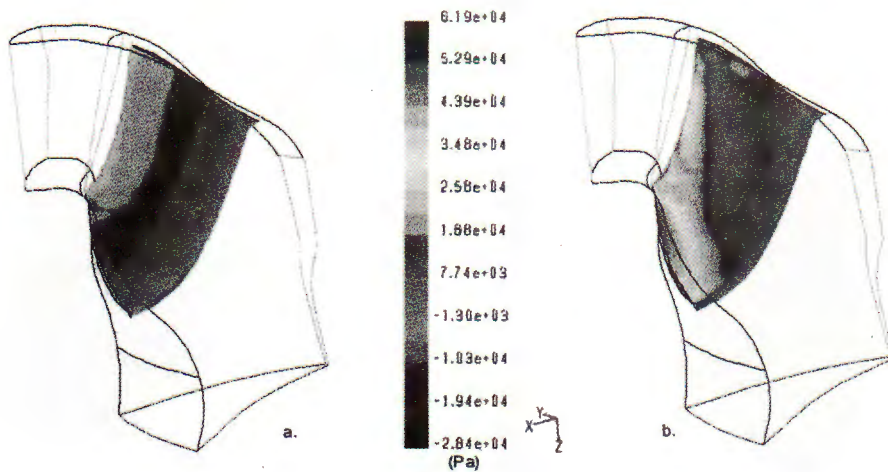


Fig. 3. Static pressure distribution on pressure side of blade at nominal (a) and runaway (b)

On the pressure side, at the off-design operating points, the relative velocity fields show that the flow is strongly perturbative on the leading edge and the hub zone, however it is almost regular on the suction side (Fig. 6). At the off-design operating points, the greatest part of kinetic moment is observed at outlet which causes a swirl and recirculation flow close to the axis of the runner which prevents to obtain experimental data in this area that is illustrated in Fig. 5 with  $R = 0$  corresponding to the center of outlet survey section. Flow surveys have been carried out with a four-holes pressure probe at the outlet section of the runner for many different operating conditions and for many radial positions. The

non-dimensional velocities are used for the comparison, defined as:

$$KC_u = \frac{C_u}{\sqrt{2gH}} \quad KC_m = \frac{C_m}{\sqrt{2gH}} \quad KC_r = \frac{C_r}{\sqrt{2gH}}$$

where  $C_u, C_m, C_r$  are respectively related to the circumferential velocity, the axial velocity and the radial velocity.

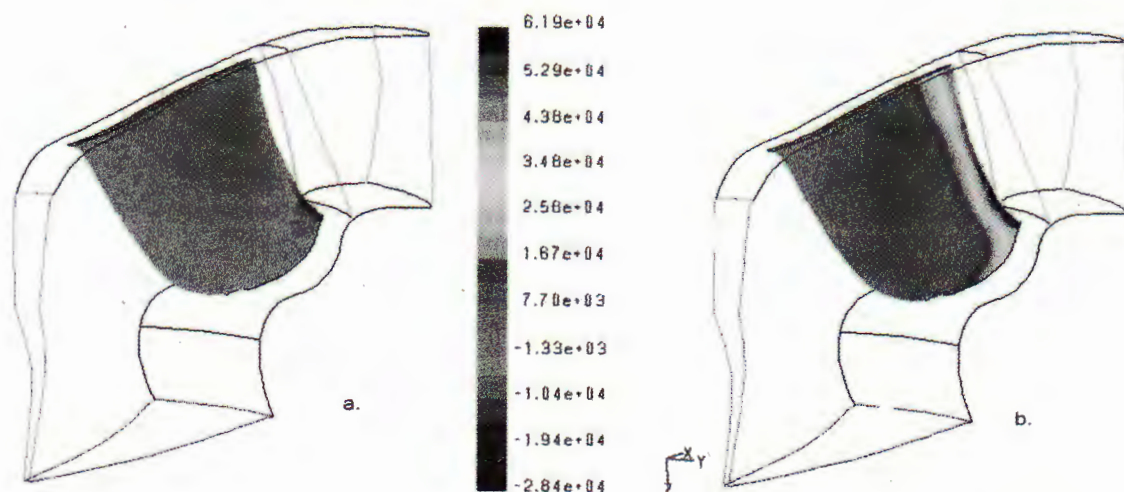


Fig. 4. Static pressure distribution on suction side of blade at nominal (a) and runaway (b)

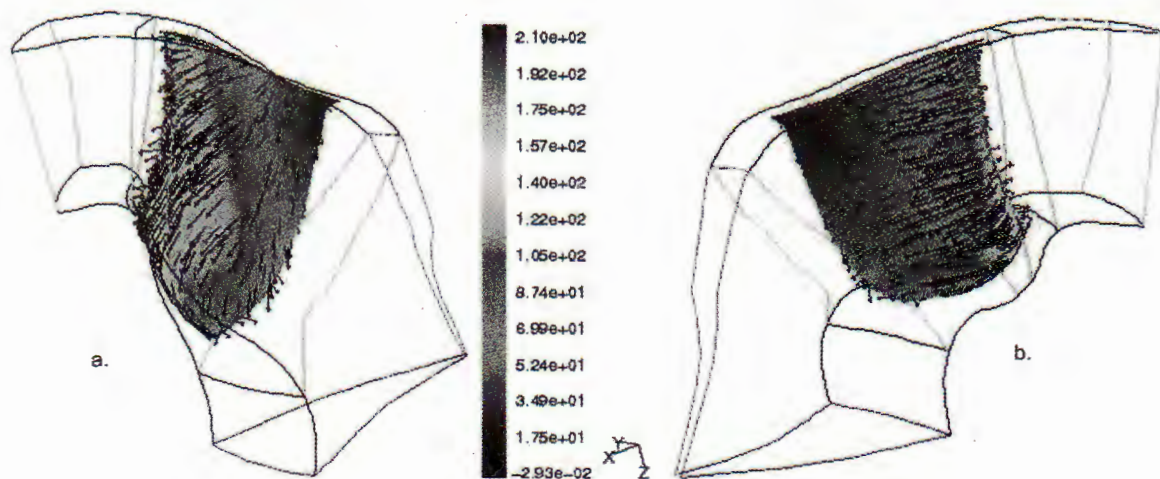


Fig. 5. Relative velocity field on pressure side (a) and suction side (b) of blade at runaway

For the outlet of the grid the numerical results coincide well with experimental flow survey. The evolution of the velocity components on the outlet is predicted for all operating points. In particular the velocity components are well predicted at the best efficiency point. However, due to the recirculation occurred in the axis zone, at the off-design points the experimental and numerical velocities are not coincided in this area (Fig. 6).

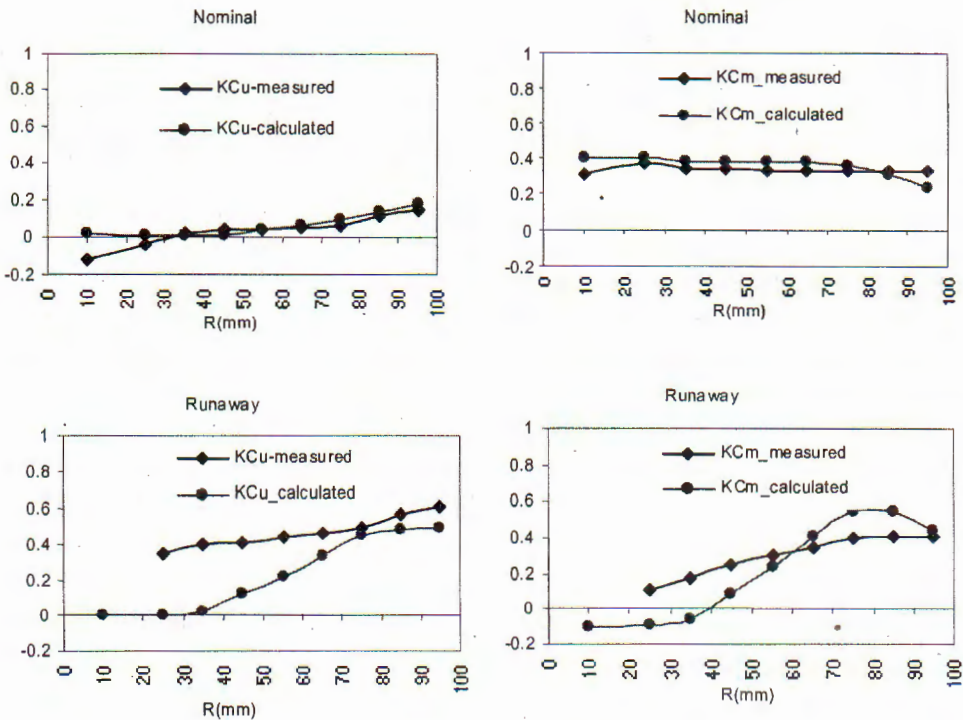


Fig. 6. Distribution of velocity components on outlet survey section

## 5 Conclusion

The calculations of the flow in a Francis turbine runner for many operating points are well performed with the industrial Navier-Stokes code (FLUENT). The mesh size is intentionally limited in order to obtain acceptable CPU times on a classical workstation. The most relevant information for the design process is well predicted such as the pressure, relative velocity evolution on blade, the moment, the numerical runaway point. Unsteady calculations provide good results with the well defined inlet boundary conditions. The evolution of velocity components is especially well calculated at nominal. For the other operating points, the velocity components is well predicted in the zone outside the recirculation. This method illustrates the capacity of the commercial code (FLUENT) for calculating the flow at nominal and even at the off-design operating points of hydraulic machines. It can then be very useful for the turbine designer to simulate the flow in the runner, then open a perspective for calculating the flow passing all components such as distributor, runner and suction pipe of a hydroelectric plant.

The present work is funded by the National Program for Fundamental Research



## References

1. Pham Thi Kim Loan, Modelisation du comportement d'une roue de turbine Francis au regime d'emballlement, *Doctoral Thesis*, INPG, France (in French), 2002.
2. Harvard Lomax, Thomas H. Pulliam, David W. Zingg, *Fundamentals of Computational Fluid Dynamics*, NASA Ames Research Center, USA, 1998.
3. FLUENT 5, *User's Guide*, Fluent Incorporated, USA, 1998.
4. Pham Thi Kim Loan, Bui Van Ga, Some results on calculation of off-design operating conditions of turbine by N3S code, *Journal of Science and Technology* **19-20** (1999) 116-120 (in Vietnamese).
5. Pham Thi Kim Loan, Bui Van Ga, A simple method of Numerical simulation of the flow in a francis turbine with interaction between components, (in Vietnamese), *National Conference on Mechanics*, Hanoi, 2002.
6. Pham Thi Kim Loan, Bui Van Ga, Numerical Simulation of the Flow in a Francis Turbine at Nominal and Off-design Operating Conditions, *HPSC in Fluid Dynamics and Technology*, Hanoi, 2003.
- 7 Pham Thi Kim Loan, Study of flow in turbine of small hydraulic central, *National Conference on Fluid Mechanics, 25<sup>th</sup> Anniversary of the Institute of Mechanics*, Hanoi, 2004.

### TÍNH TOÁN DÒNG CHẢY 3D TRONG BÁNH CÔNG TÁC TUABIN FRANCIS TẠI CHẾ ĐỘ LÀM VIỆC THIẾT KẾ VÀ NGOÀI THIẾT KẾ

Bài báo giới thiệu phương pháp sử dụng phần mềm FLUENT để tính toán dòng chảy trong bánh công tác của một tuabin Francis tại chế độ thiết kế cũng như tại các chế độ làm việc ngoài thiết kế. Từ các kết quả nhận được từ tính toán, có thể phân tích và mô tả được trạng thái dòng chảy trong bánh công tác tại các chế độ làm việc khác nhau, điều này rất có ý nghĩa trong thiết kế máy thủy khí. Giá trị các thành phần vận tốc của dòng chảy và sự phân bố áp suất trên bề mặt cánh nhận được từ kết quả tính toán phù hợp với thực nghiệm.

Chi phí thời gian máy trong quá trình tính toán và phân tích dòng chảy phải phù hợp với yêu cầu trong tiến trình thiết kế bánh công tác. Với bánh công tác được khảo sát trong bài báo này, thời gian 12 giờ để đạt hội tụ đối với bài toán tính tại một chế độ làm việc và thực hiện trên máy tính thông dụng là có thể chấp nhận được.